In Silico Genome-Scale Reconstruction and Validation of the Staphylococcus aureus Metabolic Network

Heinemann, Matthias; Kümmel, Anne; Ruinatscha, Reto; Panke, Sven

Published in:
Biotechnology and Bioengineering

Publication date:
2005

In Silico Genome-Scale Reconstruction and Validation of the *Staphylococcus aureus* Metabolic Network

Matthias Heinemann, Anne Kümmel, Reto Ruinatscha, Sven Panke

Bioprocess Laboratory, Institute of Process Engineering,
ETH Swiss Federal Institute of Technology Zurich, 8092 Zurich, Switzerland;
telepone: +41-44-6320413; fax: +41-44-6321325; e-mail: panke@ipe.mavt.ethz.ch

Received 30 March 2005; accepted 21 June 2005

Published online 9 September 2005 in Wiley InterScience (www.interscience.wiley.com). DOI: 10.1002/bit.20663

Abstract: A genome-scale metabolic model of the Gram-positive, facultative anaerobic opportunistic pathogen *Staphylococcus aureus* N315 was constructed based on current genomic data, literature, and physiological information. The model comprises 774 metabolic processes representing approximately 23% of all protein-coding regions. The model was extensively validated against experimental observations and it correctly predicted main physiological properties of the wild-type strain, such as aerobic and anaerobic respiration and fermentation. Due to the frequent involvement of *S. aureus* in hospital-acquired bacterial infections combined with its increasing antibiotic resistance, we also investigated the clinically relevant phenotype of small colony variants and found that the model predictions agreed with recent findings of proteome analyses. This indicates that the model is useful in assisting future experiments to elucidate the interrelationship of bacterial metabolism and resistance. To help directing future studies for novel chemotherapeutic targets, we conducted a large-scale in silico gene deletion study that identified 158 essential intracellular reactions. A more detailed analysis showed that the biosynthesis of glycans and lipids is rather rigid with respect to circumventing gene deletions, which should make these areas particularly interesting for antibiotic development. The combination of this stoichiometric model with transcriptomic and proteomic data should allow a new quality in the analysis of clinically relevant organisms and a more rationalized system-level search for novel drug targets.

Keywords: *Staphylococcus aureus*; genome-scale metabolic network; gene deletion; small colony variant

INTRODUCTION

Most staphylococci, Gram-positive natural habitants of skin and mucous membranes of humans, are opportunistic pathogens and are the most frequent cause for community-acquired and nosocomial infections (Novick, 2003). Their formidable ability to rapidly acquire antibiotic resistance often poses therapeutic problems. Especially *Staphylococcus aureus*, a coagulase-positive bacterium, has become a major public health threat as a result of the increased incidence of its drug resistance from penicillin/methicillin—via quinolone—to vancomycin resistance (Witte, 1999).

Various approaches are currently pursued to understand the origin of its antibiotic resistance (Lowy, 2003). Now, that the genomic sequence of this organism (Kuroda et al., 2001) as well as extensive proteomic (Cordwell et al., 2002; Hecker et al., 2003) and transcriptional data (Dunman et al., 2004; Kuroda et al., 2003) are available, it is hoped that a more holistic understanding will be achieved, consequently allowing a better identification of new drug targets.

The ultimate goal of acquiring "-omics" information is to develop a system-scale model that would allow rationally collapsing the huge amount of experimental information into a manageable (mathematical) model and thus help creating knowledge from data. This knowledge can then be used to explain a strain's physiology or to predict physiology in various real situations, particularly such that are difficult to access experimentally (such as in vivo experiments involving infections). As such an in silico model of a microorganism can be executed in minutes, it is possible to evaluate large sets of hypotheses for principle feasibility in advance, thus reducing laborious experimental series to a minimum.

En route towards a systems level model of microorganisms, genome-scale metabolic models are typically developed as a first step. Such models now exist for species such as *E. coli* (Reed et al., 2003), *S. cereviseae* (Förster et al., 2003), or *H. pylori* (Schilling et al., 2002). They exploit the vast experimental work that has been done to elucidate many aspects of organisms' metabolism, organize the information into a set of reaction equations, and thus, for example, allow appreciating the effect of deletions or additional reactions in the context of the complete (known) metabolism.

Besides representing organism-specific comprehensive metabolic compendia, stoichiometric models constitute the very basis of any in silico model describing entire cellular function (Patil et al., 2004). It was shown that already from these models—capturing only one aspect of microbial physiology—fundamental metabolic capabilities could be deduced (Price et al., 2003) and even regulatory principles

Correspondence to: S. Panke

This article includes supplementary material available via the Internet at http://www.interscience.wiley.com/jpages/0006–3592/suppmat.

could be identified (Stelling et al., 2002) by means of constraint-based modeling or pathway analysis (Papin et al., 2004). In combination with gene expression data or by addition of regulatory information (resulting in the addition or removal of pathways from the set of equations, for example through Boolean operators), the predictive power of such metabolic models can even be further enhanced (Akesson et al., 2004; Covert et al., 2004).

In addition, for pathogenic microorganisms, such a model might be useful in investigating the relationship between microbial metabolism and phenotypes that are clinically relevant and ultimately suggesting ways to exploit this knowledge in therapy. For example, a main thrust of current *S. aureus* research is concerned with mechanisms of antibiotic resistance and regulatory aspects of pathogenicity and virulence (Bronner et al., 2004; Novick, 2003; Witte, 1999). Several findings indicate that metabolic factors might play a significant role in antibiotic resistance and in the expression of virulence factors. For instance, the characteristic phenotype of small colony variants (SCV) is of high clinical relevance because it leads to particularly resistant pathogens. It is defined by a reduced growth rate and an altered pattern in carbohydrate utilization (Kohler et al., 2003; McNamara and Proctor, 2000) and thus illustrates the importance of the relationship between bacterial metabolism and the expression of virulence factors. Similarly, Somerville and co-workers stressed the importance of tricarboxylic acid (TCA) cycle activity and acetate metabolism in the context of virulence factor production (Somerville et al., 2002, 2003). Furthermore, resistance to vancomycin involves a reorganization of cell wall metabolism leading to a grossly thickened cell wall with reduced peptidoglycan cross-linking (Lowy, 2003). The redirected carbon flux towards cell wall synthesis observed in Mu50 and VM50 strains (Hanaki et al., 1998; Sieradzki and Tomasz, 1999) underlines that metabolic factors should also be taken into account when studying antibiotic resistance.

As a first step towards the systematic evaluation of metabolic factors in *S. aureus* research, we have developed a genome-scale metabolic model for *S. aureus*, more specifically using genomic information for the methicillin-resistant (MRSA) strain N315. We made use of annotations from different genomic databases, defined the biomass composition from biochemical literature, and added missing functions in order to complete specific pathways leading to certain biomass components and to represent physiological behavior. This model was validated by comparing its results to an as comprehensive set of experimental data as possible. This validated model in turn could then reproduce main physiological aspects, including for example the behavior of small colony variants, suggesting that indeed such models are useful in analyzing specific, clinically important properties. The reproductions could be further confirmed by recent expression data from the literature. Finally, we used the model to systematically search for essential genes in the *S. aureus* genome in order to guide future activities in the development of novel chemotherapeutics against essential gene products.

MATERIALS AND METHODS

Stochiometric Models and Flux Balance Analysis

A stoichiometric model is derived from mass balances for each metabolite in an organism's reaction network. At steady state, this system of mass balance equations is represented as $\mathbf{S} \cdot \boldsymbol{v} = \boldsymbol{b}$, where $\mathbf{S}$ is the stoichiometric matrix with the stoichiometric coefficients of all the metabolites in all intracellular and transport reactions, $\boldsymbol{v}$ is the flux vector containing all reaction rates $\boldsymbol{v_i}$, and vector $\boldsymbol{b}$ represents the fluxes of metabolites exchanged with the environment (i.e., the substrate uptake rates, by-product production rates). Exchange fluxes are zero for all internal metabolites, which cannot be transported across the cell membrane. Details of the procedure have been described (Stephanopoulos et al., 1998).

In addition to the mass balance equations, metabolic models generally also include constraint equations, which assign a direction to an in principle reversible metabolic reaction according to known thermodynamic constraints. These equations have the form $\alpha_i \leq v_i \leq \beta_i$, where α_i and β_i are the feasible lower and upper limits of the reaction rate v_i, respectively. For irreversible reactions, α_i is set to zero and for reversible reactions both values are typically set to arbitrarily large values. Besides defining the directions of all metabolic reactions, these constraints can also be used to specify a maximum flux through a given reaction (e.g., resulting from a limited amount of an enzyme), or to specify a measured substrate uptake rate, to include the knowledge of the minimum flux through a certain metabolic reaction, or to restrict the flux through certain reactions due to regulatory events occurring within the cell (i.e., repression of certain enzymes).

A solution of the system of mass balance equations is called a flux distribution and identifies the reaction rates in a cell with which metabolic reactions occur. However, despite the introduction of constraints and some pre-set fluxes (e.g., substrate uptake rates), the number of unknown fluxes is typically still greater than the number of mass balance equations, which leaves the system of mass balances underdetermined. Consequently, there exists a set of possible solutions (flux distributions) that can satisfy the model equations. To identify a particular flux distribution within the large set of possible solutions, linear programming optimization can be used to maximize a certain metabolic objective, implicitly assuming that the cell follows this specific rationale when selecting the particular metabolic routes that comprise bacterial metabolism under the given environmental conditions. This approach is referred to as flux balance analysis (FBA) (Varma et al., 1993). For our work, we have utilized maximization of biomass production as objective function. For solving the optimization problem, we employed the commercial software package LINDO (Lindo Systems, Chicago, IL) coupled to MATLAB (Mathworks, Natick, MA).

For in silico modeling experiments, also a growth medium has to be defined. Unless otherwise stated, we employed a

minimal in silico medium consisting of glucose as carbon/energy source, water, metal ions, nitrogen, phosphate and sulfur sources, and nicotinate. These components were allowed to enter and leave the cell unrestrained. Exchange fluxes for compounds present in the in silico medium were constrained to positive values (i.e., limited to influx). For metabolites that are capable of leaving the cell (i.e., acetate, lactate, carbon dioxide, etc.), the exchange fluxes were constrained to negative values (i.e., limited to efflux).

DEVELOPMENT OF STOICHIOMETRIC METABOLIC MODEL

Stoichiometric metabolic models can be constructed using data from different sources. In this work, the development of the model comprised three distinct steps: (i) exploitation of genomic databases to construct a first system of mass balances for the catabolic reactions that lead to the formation of metabolites (monomers for nucleic acids, proteins, cell envelope components, and the pool of solutes inside the cell) and anabolism; (ii) definition of reactions for polymer and biomass formation and maintenance requirements; (iii) completion of the model with data from the biochemical literature and from other database sources, resulting in the addition of functions not available from the genomic databases but obviously required by biomass composition or physiological needs.

For the first step (i), specifically information for the strain N315 was employed, while for the steps two (ii) and three (iii), due to the scarcity of experimental data specifically for N315, data were also taken from other *S. aureus* strains with the underlying assumption that the genome-based metabolic capabilities of the various strains are conserved.

Exploitation of Genome Annotations

The KEGG database (http://www.genome.jp/kegg/) was taken as starting point for model building, since in this database the gene annotation of every sequenced strain is linked to its functions. From this database, the respective data for *S. aureus* N315 were downloaded and corrected for obvious errors (such as the infrequent occurrence of different names for the same metabolite). As commonly done with metabolic models, we did not account for the distinction between α- and β-sugars (Reed et al., 2003). In this first model reconstruction step, information about reversibility or irreversibility of reactions was also taken from the KEGG database using its reaction network maps that represent several metabolic subsystems. Where identical reactions were included in several maps but with different directions, the reversible case was chosen for our model.

To further complement the KEGG reaction network, we used the TIGR database (http://www.tigr.org). Being based on the same sequence data, this database runs a different annotation methodology. There is a large overlap between these two databases. Metabolic functions additionally identified by the TIGR annotation (on the basis of completely assigned EC numbers) were added to our model.

To link the reconstructed intracellular metabolism with the external environment, analogously to the reactions of the intracellular metabolism, the information on transporters were taken from the KEGG as well as from the TIGR database and supplemented with the corresponding reactions from the Transport Classification Database TC-DB (http://tcdb.ucsd.edu).

Due to the advent of the genomic sciences and the accompanying development of powerful bioinformatics tools and databases, a large part of the metabolic model can be reconstructed from gene annotations. However, today's data quality and the limited inter-database compatibility are not sufficient to establish a metabolic model by exclusively using genomic annotation databases such as KEGG or TIGR. Large portions of the network, whose presence is demanded from the biochemical literature or by simple logic are frequently absent from the sequence annotations (Iliopoulos et al., 2000). Therefore, a substantial part of the model building is the manual reconstruction of reactions from literature, especially in genome regions where limited homology on amino acid sequence level makes gene function assignment difficult. Two examples of this are given in the Results section.

Definition of Biomass Constituting Equations and Energy Requirements

For any genome-scale metabolic model, a set of biomass constituting reactions has to be formulated. This set consists of reactions converting specific metabolites (monomers) into polymers (including a formal reaction considering the pool solutes) and a final reaction converting these polymers into biomass. In our model, the five polymer categories DNA, RNA, proteins, lipids, and cell wall plus the pool of solutes were used. According to their experimentally determined weight fractions in the cellular biomass, these polymers were then joined together into a final biomass constituting reaction. ATP consumption for synthesis of RNA, DNA, and proteins also had to be taken into account. As there is no specific information available for the energy requirements for *S. aureus*, values for *E. coli* were used (Ingraham et al., 1983).

No data on biomass composition were available specifically for strain N315. Thus, literature data originating from a variety of *S. aureus* strains had to be employed assuming similarity between the *S. aureus* in general and the strain N315. However, data on the strains' biomass composition were obtained under a variety of growth conditions using a large number of different (typically complex) media. As the biomass composition depends on medium composition and growth condition, the available data sets were not coherent. Through the vast amount of available data (see supplementary information), however, it was possible to derive a representative average biomass composition of a *S. aureus* strain (cf. Table I). As it has also been shown that FBA results are not very sensitive to variation in biomass composition

Table I. Metabolites considered to be required for biomass generation in *S. aureus*.

Protein (0.4 g protein/g CDW)	mmol/g protein
Alanine	0.492
Arginine	0.268
Asparagine	0.433
Aspartate	0.446
Cysteine	0.048
Glutamine	0.318
Glutamate	0.497
Glycine	0.462
Histidine	0.178
Isoleucine	0.658
Leucine	0.699
Lysine	0.576
Methionine	0.202
Phenylalanine	0.343
Proline	0.246
Serine	0.469
Threonine	0.443
Tryptophane	0.057
Tyrosine	0.298
Valine	0.514
ATP (polymerization energy)	39.94
DNA (0.03 g DNA/g CDW)	mmol/g DNA
dATP	0.676
dCTP	0.33
dGTP	0.33
dTTP	0.676
ATP (polymerization energy)	4.39
RNA (0.12 g RNA/g CDW)	mmol/g RNA
ATP	0.506
CTP	0.496
GTP	0.496
UTP	0.506
ATP (polymerization energy)	1.25
Lipids (0.07 g lipids/g CDW)	mmol/g lipid
Phosphatidylglycerol	0.4588
Cardiolipin	0.0574
Lysylphosphatidylglycerol	0.0574
Menaquinol/Menaquinone	0.0765
Lipoteichoic acid	0.0344
Diglucosyl-dihexadecanoylglycerol	0.0688
3-D-Glucosyl-1,2-dihexadecanoylglycerol	0.0115
1,2-Dihexadecanoyl-*sn*-glycerol	0.1912
Cell wall (0.24 g cell wall/g CDW)	mmol/g cell wall
Crosslinked peptidoglycan	0.363
Teichoic acid	0.019
Pool solutes (0.14 g pool/g CDW)	mmol/g pool
Alanine	0.1161
Arginine	0.0288
Aspartate	0.5959
Glutamate	0.5256
Glutamine	0.0086
Glycine	0.0398
Histidine	0.0169
Isoleucine	0.0481
Leucine	0.0222
Lysine	0.0405
Methionine	0.0222
Phenylalanine	0.0043
Proline	0.1293
Serine	0.0756
Threonine	0.0156
Tryptophane	0.0017
Valine	0.0162
ATP	0.0008
K^+	13.3495
Mg^{2+}	0.8953
Na^+	1.9895
Orthophosphate	0.9947
D-Glucose equival	0.4775
Acetyl-CoA	0.00033
Succinyl-CoA	0.00002
CoA	0.0004
FAD	0.00067
NAD^+	0.01433
NADH	0.00033
$NADP^+$	0.00087
NADPH	0.00267

Note: An average chain length of the fatty acids of 16 was used as sole representative for all acyl-chains based lipids.

References for the biomass composition can be found with the supplementary material.

(Pramanik and Keasling, 1998), this averaged biomass composition was used for all our simulations.

DNA/RNA

The ratio of the nucleic acids in the DNA was derived from the G/C-content according to the genome sequence (Kuroda et al., 2001). The RNA nucleic acid composition was also determined from the genome's G/C-content assuming that the ratios of G to C and A to U are unity.

Proteins

For the protein assembly reaction, the average amino acid composition was taken from a genomic sequence-based analysis (http://www.pasteur.fr/~tekaia/aafreq_GENE.html).

Lipids

The most prominent lipids occurring in *S. aureus* are phospholipids, glycolipids, and apolar lipids (Wilkinson, 1997). The phospholipids are phosphatidyl glycerol, cardiolipin, and lysyl-phosphatidyl glycerol (Hugo and Davidson, 1973; Koch et al., 1984; O'Leary and Wilkinson, 1988; White and Frerman, 1967). There are three glycolipids reported: monoglycosyldiacyl glycerol, diglycosyldiacyl glycerol, and lipoteichoic acid (Hugo and Davidson, 1973; White and Frerman, 1967). The major apolar lipid is menaquinone (White and Frerman, 1967). Furthermore, there is evidence on the presence of considerable amounts of 1,2-diacylglycerol (Koch et al., 1984).

For acylglycerol-based compounds such as phospholipids, glycolipids, and 1,2-diacylglycerol, an average fatty acid chain length of 16 was calculated from experimental data and an unsaturation of the fatty acids was neglected since it was shown that only less than 5% of the chains have a C-C-double bond (Gutberlet et al., 2000; Hugo and Davidson, 1973; O'Leary and Wilkinson, 1988; Ward and Perkins, 1968; Weerkamp et al., 1978).

Cell Wall Constituents

The cell wall constitutents of *S. aureus* include murein (Tomasz, 2000; Weidel and Pelzer, 1964), teichoic acids (Baddiley, 1989), and wall-associated surface proteins (Perry et al., 2002). The latter have already been considered in the protein section. The lipoteichoic acids, that is teichoic acids attached to the membrane lipids, were included in the lipid fraction as they were determined experimentally as a part of this fraction (Koch et al., 1984). They are synthesized via a different pathway than wall teichoic acid and differ structurally, too (cf. Fig. 1). The wall teichoic acids, linked to peptidoglycan, and peptidoglycan itself, constitute the ''polymer'' cell wall.

Pool of Solutes

The pool of solutes includes mainly free amino acids (Graham and Wilkinson, 1992; Hancock, 1960; Miller et al., 1991; Tynecka, 1968) and metal ions (Christian and Waltho, 1964; Graham and Wilkinson, 1992) with potassium as the predominating ion (Wilkinson, 1997) and carbohydrates expressed in glucose equivalents (Miller et al., 1991). Intracellular concentrations of ATP were taken from the literature (Vinnikov, 1988), while concentration data for the remaining pool components (acetyl-CoA, succinyl-CoA, CoA, FAD, NAD(H), NADP(H)) were taken from *E. coli* as they were unavailable for *S. aureus* (Pramanik and Keasling, 1997; Reed et al., 2003). It is important to note that when a medium with high osmolarity is employed, glycine betaine should be added to the pool of solutes, since it is known that *S. aureus* uses this compound as pool component in high amounts for osmoregulation (Graham and Wilkinson, 1992; Miller et al., 1991).

Biomass Synthesis and Maintenance Requirements

The above-mentioned polymers are combined into a single reaction leading to the formation of biomass. The weight fraction of each polymer was determined based on a number of different literature sources (Christian and Waltho, 1964; Hugo and Davidson, 1973; Wilkinson, 1997; Wiltshire and Foster, 2001).

Not all consumed substrate is used for synthesis of new biomass and energy production, but some effort is also essential to maintain the cell's integrity. In our model, all maintenance efforts are ''paid'' for with ATP as energy currency, which is in agreement with the current practice in the field (Varma et al., 1993). The ATP maintenance requirements are typically divided into a growth-associated and non-growth associated part (Chen, 1964; Tempest and Neijssel, 1984). The growth-associated portion is normally considered in the overall biomass equation by an additional conversion of ATP and water into ADP and orthophosphate. For the non-growth associated maintenance requirements, an ATP drain flux is defined constantly removing ATP at a fixed rate.

The respective values for growth-associated and non-growth associated ATP maintenance requirements are normally determined experimentally. Knowing the stoichiometry of ATP production and by measuring substrate uptake rates at varying growth rates, both parameters can be determined (Stephanopoulos et al., 1998). To the best of our knowledge, such data are not available for staphylococci. Experimentally determined maintenance parameters for different organisms show that values of 40 mmol ATP/(g cell dry weight)/h and 5 mmol ATP/(g cell dry weight) for growth-associated and non-growth associated maintenance requirement are reasonable assumptions, corresponding to an ATP consumption of about 70 mmol ATP/(g cell dry weight)/h (Stephanopoulos et al., 1998).

Completion of the Model With Data From Various Sources

Network gaps remaining after exploitation of genomic databases were closed with reactions derived from a number of different sources. Missing reactions in pathways leading to metabolites for polymers were identified by the use of linear programming methods, in which metabolite production was maximized. For the generation of hypotheses on the missing of certain metabolic functions, reactions from the set of KEGG reference pathways were systematically added and it was checked whether the consequent synthesis of the respective metabolite was possible. None of the reactions identified to be able to fill certain network gaps could be inferred from the KEGG genome annotations of any of the other available *S. aureus* genome sequences. Thus, the identified reactions were screened against putatively assigned enzymes from KEGG and TIGR, which had not been included in the model until then. The SEED-WIT2 database (http://wit.mcs.anl.gov/WIT2/) supported comparative analysis of so far missing functions.

To the largest extent, however, biochemical data from literature were used to complete the model by adding enzymes and reactions specifically occurring in *S. aureus* strains. In addition to this, additional and so far biochemically not yet identified reactions had to be inserted in order to allow for an in silico representation of in vivo observed physiological behavior. In this context, especially transporters were added.

Finally, the preliminary set of reaction directions, taken from the KEGG database, had to be carefully revised, as the initial set of suggested reaction directions allowed certain cycle fluxes, which produced ATP without net conversion of any other metabolite or permitted an artificial transhydrogenation by converting NADH into NADPH. We changed 30 so far reversible to irreversible reactions in order to avoid these thermodynamically infeasible flux states or the artificial transhydrogenation cycles.

Charge and elementally balancing of the reaction network was omitted as the therefore required additional efforts

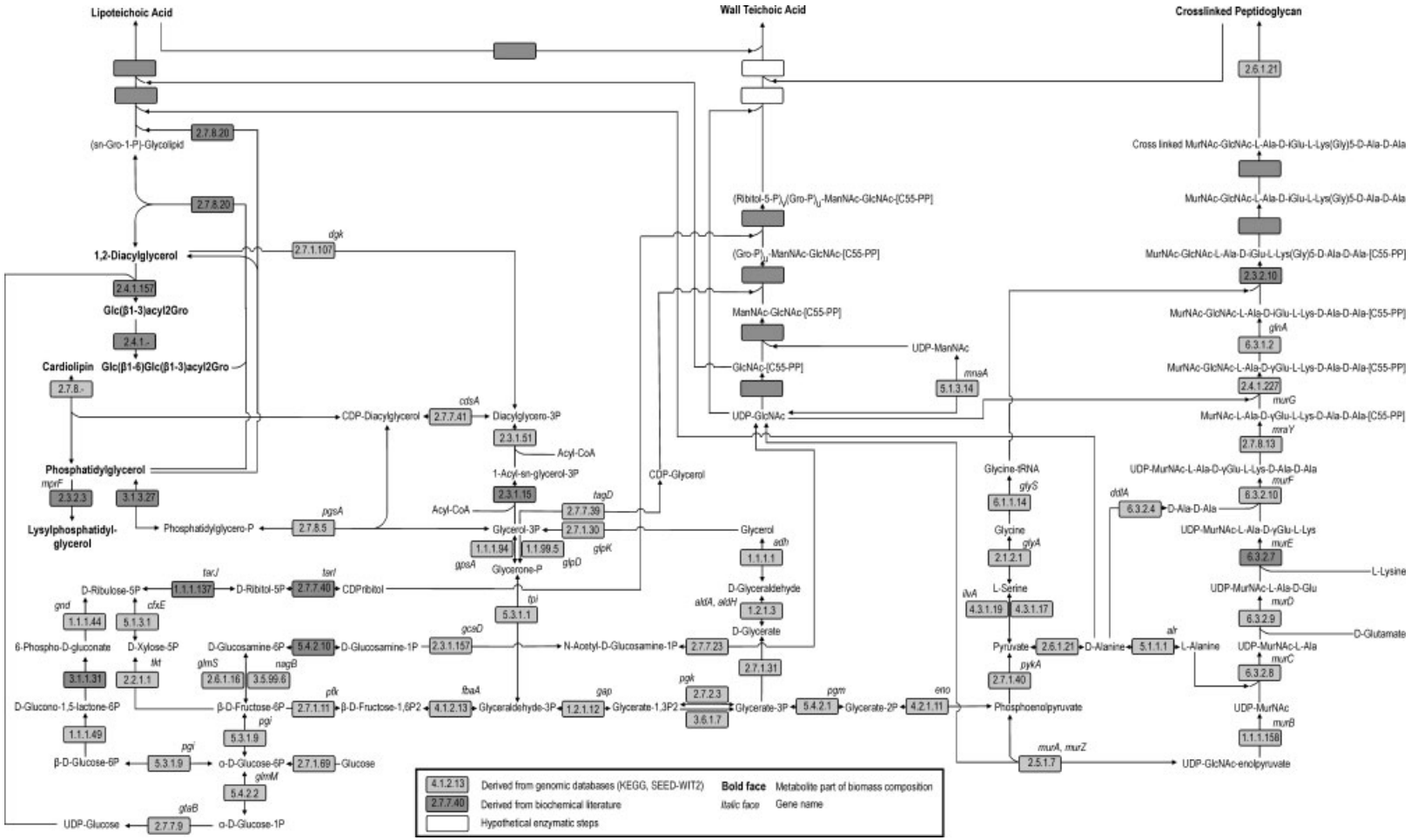

Figure 1. Illustration of the reconstructed pathways leading to cell envelope constituents. Abbreviations were taken from the KEGG database. C55-P denotes the undecaprenol phosphate lipid carrier. The following biochemical literature sources were employed for reconstruction: (Arakawa et al., 1981; Blumenthal, 1972; Harrington and Baddiley, 1985; Ito and Strominger, 1962; Jolly et al., 1997; Kiriukhin and Neuhaus, 2001; Koch et al., 1984; Navarre and Schneewind, 1999; Perego et al., 1995; Pereira and Brown, 2004).

would not have provided a proportional enhancement of results.

The complete model (including the sources or references for every reaction including gene names) is available for download from the supplementary files.

RESULTS

Model Characteristics

In the following, general properties of the reconstructed network are presented in order to allow for an appraisal of the completeness of the metabolic model.

The in silico metabolic genotype of *S. aureus* enables 774 metabolic processes (682 internal processes and 92 transport processes) that influence 712 metabolites. There are 604 enzymes involved, of which 551 have ORF assignments in the sequence annotations of either KEGG (including the database's section of only putatively assigned functions), TIGR, SEED-WIT2, or the primary annotation (Kuroda et al., 2001), while the remaining 48 enzymes have not been assigned to genes but were added to the model due to biochemical evidence or physiological considerations (Tables II and III). Table II provides a quantitative summary of the sources of the metabolic processes comprising internal, transport, biomass-constituting and maintenance as well as spontaneous chemical reactions.

The genome sequence of *S. aureus* N315 is known to have a length of 2,813,641 base pairs with an estimated 2595 protein-coding regions (Kuroda et al., 2001). Thus, our metabolic model covers approximately 23% of all ORFs, assuming that every added and not yet assigned enzymatic function is encoded in a single gene. In accordance with the recently proposed nomenclature for in silico metabolic models (Reed et al., 2003), the model is termed iMH551, where 551 represents the number of genes involved in the model with a so far known locus in the genome.

A total of 248 metabolites (approx. 35% of all metabolites) were found to be involved in only one reaction. In other words, they were only consumed or only produced, but not both. Reasons for this could be that connecting reactions were not yet identified, proteins may have been assigned a wrong function, or *S. aureus* N315 has lost specific functions through evolution. Part of this relatively large portion is likely to be a result of the still incomplete genome annotation. The core model without dead-end pathways comprises 549 reactions with 410 metabolites. By addition of 11 auxiliary reactions (i.e., the biomass constituting and maintenance reactions) and the corresponding eight auxiliary metabolites (including the polymers), the model was completed in terms of biomass assembly and ATP maintenance requirements.

Table II. Sources of in silico metabolic processes.

Total metabolic processes	774
Enzymatic and transport reactions	756
Genomic databases matches	708
KEGG	663
TIGR	29
SEED-WIT2	8
Primary annotation (Kuroda et al., 2001)	8
No genomic database matches	48
Biochemical literature	34
Physiological literature	2
Added reactions	12
Spontaneous chemical reactions and transport phenomena	7
Biomass constituting and ATP maintenance reactions	11

Table III. Distribution of reactions of *S. aureus* with currently no ORF assignment that were added during the reconstruction process.

Metabolism	No. of reactions
Amino acid metabolism	1
Carbohydrate metabolism	7
Energy metabolism	6
Glycan biosynthesis and metabolism	11
Lipid metabolism	16
Membrane transport	3
Metabolism of cofactors and vitamins	3
Nucleotide metabolism	1

Reconstruction of Pathways to Cell Envelope Constituents

The *S. aureus* cell wall is known to be important in the context of antibiotic resistance (Kuroda et al., 2003; Pechous et al., 2004). Furthermore, as metabolic alterations affecting the cell wall structures have been described in this context (Cui et al., 2000), this motivated us to put a special focus on this part of the metabolic network.

Reconstructing cell wall and cell membrane metabolism in particular was strongly hampered by incomplete or even completely missing pathway assignments from genomic databases. In this respect it is important to note that such homology approaches strongly depend on the degree of enzyme and pathway conservation and might not be useful to describe specialized metabolic pathways of a particular strain. Looking at Gram-positive bacteria, pathway variability is particularly obvious in the context of cell wall composition, for example the composition of the lipoteichoic and wall-teichoic acids differs with the genus (Neuhaus and Baddiley, 2003; Reusch, 1984; Sutcliffe and Shaw, 1991). Thus, the reconstruction of *S. aureus* metabolic pathways leading to these cell wall residues was mainly established using biochemical literature and not with the aid of genomic databases. On the other hand, pathways leading to peptidoglycan precursors, which are rather well conserved within Gram-positives (Schleifer and Kandler, 1972), could be readily reconstructed from genomic databases.

By including information from an additional genomic database (SEED-WIT2) as well as by adding functions required by the cell envelope's composition, it was possible to develop an overall metabolic picture for the main cell envelope constituents (Fig. 1). Incorporations of additional functions included (i) a hypothetical enzymatic step in place

of the still unknown enzymatic machinery required for wall-teichoic acid attachment to glycan strands (Navarre and Schneewind, 1999) and (ii) another hypothetical enzymatic step to include wall-teichoic acid glycosylation (Harrington and Baddiley, 1985; Neuhaus and Baddiley, 2003).

The quality of this part of our model was confirmed by flux balance considerations. Predictions of flux distributions in the pathways to cell envelope constituents under aerobic conditions with a complex medium containing glucose as the main carbon source were in good agreement with experimental results. For example, we calculated a 94% incorporation of the glycerophosphate moieties of phosphatidylglycerol into lipoteichoic acid polymers, whereas 90% were described in pulse-chase experiments. Furthermore, we predicted that 8% of 1,2-diacylglycerol are used for the synthesis of glycolipids and the lipid anchor of lipoteichoic acids in comparison to the experimentally determined 10% (Koch et al., 1984).

Overall, with the model we can present an expanded view of the *S. aureus* cell envelope metabolism linked to the entire cellular metabolism. This is in stark contrast to common attempts focused on localized aspects of distinct cell envelope structures (Navarre and Schneewind, 1999; Neuhaus and Baddiley, 2003).

Reconstruction of the Respiratory Chain

As *S. aureus* is capable of growing aerobically, a fully functional respiratory chain, including membrane-associated dehydrogenases, quinone electron transfer, and ATPase had to be reconstructed (Fig. 2). The KEGG sequence annotation of *S. aureus* N315 identified several genes encoding respiratory chain dehydrogenases. These dehydrogenases oxidize NADH, L-lactate, succinate, glycerol 3-phosphate, (S)-malate, and formate. In most cases, however, we were unable to identify the according electron acceptors from the KEGG sequence annotation. Thus, these reactions were carefully revised using data from biochemical literature (Kubak and Yotis, 1981; McNamara and Proctor, 2000; Sehnalova and Dadak, 1976; Tynecka and Malm, 1996; Tynecka et al., 1999; Wilkinson, 1997). As menaquinone is known to be the only quinone in *S. aureus* (McNamara and Proctor, 2000 Tynecka et al., 1999; Wilkinson, 1997), the ubiquinone dependency of the NADH dehydrogenase, erroneously identified by the KEGG annotation, was substituted by a menaquinone dependency (NDH I) (Tynecka et al., 1999). From the biochemical literature, the list of sequence derived primary electron donors was further supplemented by a menaquinone-dependent $FADH_2$ dehydrogenase (McNamara and Proctor, 2000; Wilkinson, 1997) and a lactate dehydrogenase with the same electron acceptor (Tynecka et al., 1999).

Electron transfer to the terminal electron acceptor is mediated by two terminal oxidases ($ba_3(a_{602})$- and $bo(b_{556})$-type) that use *b*-type cytochromes as interim electron carriers (Tynecka et al., 1999). They are collapsed into one step in the model and also in Fig. 2. According to studies carried out with *S. aureus* 17810R, the NADH dehydrogenase and the cytochrome *b* oxidase are translocating protons across the membrane to establish the proton motive force (PMF) (Tynecka et al., 1999). As the details of the molecular mechanisms of the two proton-translocating enzymes are not available, we assumed that in both cases two protons are translocated.

The efficiency of the ATPase in *S. aureus* (F_0F_1) in using the PMF to generate ATP was calculated from a literature-derived experimentally determined PMF (Kashket, 1981). According to the chemiosmotic theory, the H^+/ATP stoichiometry was calculated from the comparison of the PMF and the phosphorylation potential. Applying experimental data on ATP, ADP, and P_i concentrations for growing *S. aureus* cells (Christian and Waltho, 1964; Tynecka et al., 1999) and on Gibbs free energy of formation of these compounds under physiological conditions (Alberty, 2000),

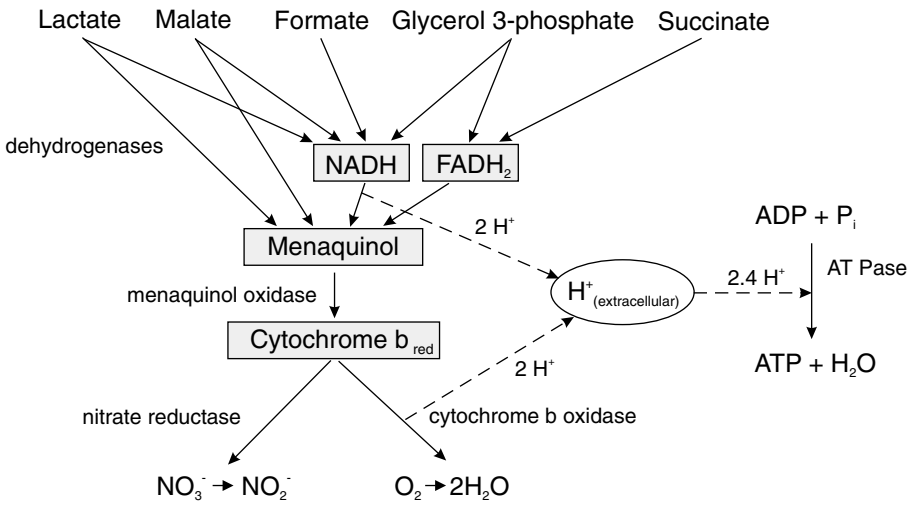

Figure 2. Scheme of the reconstructed respiratory chain. Solid lines represent enzymatic reactions, whereas broken lines denote proton translocation processes. Only the reduced forms of the metabolites are given in the figure.

it was calculated that 2.4 protons have to be transported across the membrane to synthesize one molecule of ATP. The fact that this thermodynamically determined stoichiometry is a non-integer number is in agreement with the literature on other microorganisms, for example *E. coli* (Jiang et al., 2001). It results from the fact that the ratio of *c* subunits in the H^+ transporting F_0 rotary motor (which is still unknown for the *S. aureus* ATPase) and the three ATP molecules produced per complete rotary movement of the $\alpha_3\beta_3$ hexamer of the F_1 complex is not necessarily an integer number. *E.coli*, for example, has ten *c* subunits, which consequently lead to a H^+/ATP stoichiometry of 3.3 (Jiang et al., 2001). In summary, with the values we have assigned for the proton translocation in the respiratory chain and the one determined for the H^+/ATP stoichiometry, approximately 1.7 molecules of ATP are produced per molecule of NADH (with NADH-linked substrates), which is in reasonable agreement with the generally assumed ratio of 2 for *S. aureus* (Wilkinson, 1997) and with the only known experimental *S. aureus* P/O ratio of 1.3 determined for glutamate as a substrate (Tynecka et al., 1999).

Under anaerobic conditions, *S. aureus* is able to grow by fermentation of a carbohydrate carbon source to lactic acid or by anaerobic respiration by utilizing nitrate as the terminal electron acceptor (Burke and Lascelles, 1975). In the latter case, cytochrome-*b* (Burke et al., 1981; Burke and Lascelles, 1979; Lascelles and Burke, 1978) and menaquinone (Sasarman et al., 1974) take part in the electron transport chain and we assumed that the nitrate reductase is not involved in proton translocation.

Prediction of Phenotype Characteristics

With the reconstructed metabolic network, it should now be possible to predict certain phenotypic characteristics using the FBA approach. We used maximization of bacterial biomass production as objective function for FBA, as it has been shown for *E. coli* that the cell's regulatory machinery indeed controls the metabolic fluxes to achieve maximal biomass per consumed substrate (Burgard and Maranas, 2003), and fixed a substrate uptake rate. Then FBA allows calculating the value of all metabolic fluxes. These represent in principle the enzymatic reaction rates at the organism's optimum flux distribution for biomass production. In this context, it is important to note that typically alternative optimal solutions exist for the internal flux distribution (Mahadevan and Schilling, 2003). In the following, examples of predicted physiological phenotypes will be presented, for which it was checked that the general result is not influenced by flux variability.

Minimal Requirements

S. aureus N315 is capable of synthesizing all amino acids, since the complete set of genes for the corresponding biosynthesis pathways has been annotated in the genome (Kuroda et al., 2001). An auxotrophy for several amino acids, sometimes observed with staphylococci isolated from their hosts, is commonly explained by a repression of the corresponding pathways. These auxotrophies, however, can be eliminated by successively reducing the number of amino acids in the medium (Gladstone, 1937). Accordingly, the in silico organism has no ''intrinsic'' auxotrophy for any amino acid.

With the model, however, an auxotrophy is predicted for nicotinate for the synthesis of NADH and NADPH. This is in agreement with the literature, while the described requirement of thiamin or biotin is not reproduced by the model (Gladstone, 1937; Kuroda et al., 2001; Miller and Fung, 1973). This is due to the fact that in our model these two B-group vitamins, representing prosthetic groups for a number of proteins, are not considered in the biomass composition. However, this does not have an impact on the results presented in the following.

In the model, sulfate, ammonia, and inorganic phosphate are used as sources of sulfur, nitrogen, and phosphorus, respectively. Furthermore, the in silico organism requires magnesium, sodium, and potassium ions due to the fact that these are included in the pool of solutes. In experiments, these metal ions are also typically added to the medium (Gladstone, 1937; Miller and Fung, 1973; Wu and Bergdoll, 1971).

Aerobic and Anaerobic Growth

Under anaerobic conditions, *S. aureus* is able to grow by fermentation of, for example, glucose to lactate or by anaerobic respiration with nitrate as terminal electron acceptor (Blumenthal, 1972; Burke and Lascelles, 1975; Throup et al., 2001). FBA of fermentative growth on glucose minimal media shows that the in silico organism is unable to synthesize nucleic acids and consequently also DNA or RNA. The calculation suggested that this shortcoming could be compensated by addition of uracil to the medium. This behavior has been confirmed experimentally (Burke and Lascelles, 1975; Garrard and Lascelle, 1968; Kashket, 1981; Wilkinson, 1997). In the following, uracil is added to the in silico medium.

The experimentally observed main fermentation product with *S. aureus* is lactate. It is generated by the reduction of pyruvate with the NADH-dependent lactate dehydrogenase, thereby, recycling NAD^+. Under respiratory conditions, NADH recycling is achieved by the various dehydrogenases belonging to the respiratory chain. Here, an excellent agreement in terms of by-product formation was found between the experimental data and the simulation. Figure 3A illustrates the major fluxes of *S. aureus* growing anaerobically on glucose.

It was shown experimentally that the anaerobic respiration uses the same apparatus as the aerobic respiration (e.g., menaquinone and cytochrome-*b* as electron carriers) (Lascelles, 1979; Lascelles and Burke, 1978; Sasarman et al., 1974). Also, the model predicts that the flux distribution for

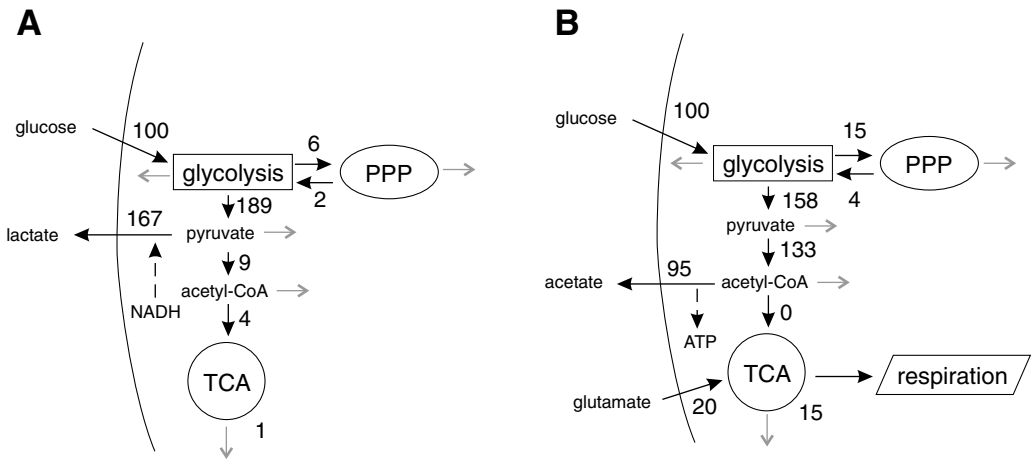

Figure 3. Illustration of major fluxes of *S. aureus* growing anaerobically on glucose medium without nitrate (**A**) and growing aerobically on medium with glucose excess and glutamate (simulated as *acnA* mutant) (**B**). Fluxes are given relative to the specific glucose consumption rate. TCA: tricarboxylic acid cycle; PPP: pentose phosphate pathway.

anaerobic respiration is similar to the one for aerobic respiration with the difference that nitrate reductase instead of cytochrome-*b* oxidase is used to transfer electrons to the terminal electron acceptor.

Under aerobic conditions, *S. aureus* utilizes glycolysis, pentose phosphate pathway, and TCA cycle to catabolize glucose (Blumenthal 1972). An excess of this particular carbon source, however, leads to repression of the TCA cycle activity and excretion of acetate (Blumenthal, 1972; Somerville et al., 2002, 2003). This behavior, known as ''glucose effect,'' cannot be simulated with FBA using growth maximization as objective function as the secretion of not completely oxidized carbon will result in a reduction of biomass yield. This contradicts the given FBA objective function. In a rich carbon source environment, however, maximization of biomass yield might be less important and other objectives may be more favorable for the cell (e.g., inhibition of competing bacteria in the body). As the true objective for this glucose effect remains elusive, we included its manifestation (downregulation of TCA activity) by constraining fluxes. In this particular case, we constrained the flux through the acontinate hydratase reaction (encoded by *acnA*) for aerobic conditions and glucose excess. Release of acetate into the medium was then also observed in silico. An experimental analysis of an *acnA* mutant supported this approach: During the exponential growth phase, no significant difference in growth rate between the *acnA* mutant and the wild-type strain was observed (Somerville et al., 2002), which is completely in line with the prediction of the adapted model (although the model predicts an additional glutamate auxotrophy for the mutant, which would have remained undetected in the experiment because of complex medium). Figure 3B illustrates the major fluxes of the wild type (simulated as *acnA* mutant) growing with glucose excess.

The presented results demonstrate that the model is capable of reproducing the main characteristics of aerobic and anaerobic growth as described in the experimental literature. An exact comparison of yields or growth rates was impossible because in most cases experimental data were obtained with complex media, of which the exact chemical composition was unknown. For an exact comparison of yields, however, the medium composition has to be known, whereas for a prediction of growth rates also experimentally determined substrate uptake rates are necessary, which are also not available from the literature.

Nevertheless, by-product formation as well as the requirement of additional medium components is either correctly predicted with our model using FBA with growth maximization as objective function or can be easily accounted for. This indicates that also for *S. aureus* this objective function is in most in vitro cases applicable as it has been shown for *E. coli* (Burgard and Maranas 2003).

Small Colony Variants

Having validated our model against the available experimental evidence, we proceeded to analyze a clinically relevant phenotype. Small colony variants (SCV) of *S. aureus* have been the focus of several studies because of a close association between the recovery of SCV and infections (Kohler et al., 2003; McNamara and Proctor, 2000). SCV show an alteration in metabolism leading to slow growth. It has been suggested that this is mainly caused by the interruption of the electron transport chain (Proctor et al., 1994). To analyze small colony variants experimentally, *hemB* mutants were constructed (Kohler et al., 2003; McNamara and Proctor, 2000; von Eiff et al., 1997). These mutants lack the ability to synthesize heme and thus mimic SCV with their interrupted electron transport chain. As the SCV phenotype is experimentally rather well defined, we investigated whether our model could faithfully reproduce the observed behavior by simply removing the heme-requiring cytochrome-*b* oxidase from the model.

When aerobic conditions and a mineral medium with glucose were assumed for the in silico *hemB* mutant, we found an essentially fermentative behavior: lactate excretion and consequently reduced growth rate. Correctly, the in silico *hemB* mutant did not show nitrite accumulation after nitrate addition as found experimentally (Burke and Lascelles, 1975). As a next step, we added systematically all proteinogenic amino acids, for which *S. aureus* can provide a transporter to the nitrate-free medium separately and investigated their effect on growth rate. According to the model, glutamate, glutamine, and arginine should lead to an increase in growth rate because of additional energy production. Isoleucine, leucine, valine, and lysine should be utilized directly for polymer synthesis (also leading to a growth rate increase), whereas glycine and alanine should not be consumed at all. The last effect is a result of the fact that the transport of these two amino acids into the cell is under these specific modeling conditions energetically more costly than the potential gain by avoided biosynthesis.

Looking more detailed at the effect of glutamate, glutamine, and arginine in the medium, the model predicted that arginine would be used for protein synthesis and ATP production (via the breakdown of carbamoyl-phosphate obtained from citrulline), explaining the effect on growth rate. Remarkably, this is very much in line with protein expression studies that showed an increase in the level of the enzymes of the arginine deiminase pathway together with the level of glycolytic enzymes in a *hemB* mutant during anaerobiosis (Kohler et al., 2003). From the experimental study, it was postulated that arginine was depleted to finally produce ATP (Kohler et al., 2003).

Furthermore, the model predicted that glutamate and glutamine would increase biomass yields by ATP production. In these cases, acetate is excreted via pyruvate oxidase and acetate kinase with concomitant formation of ATP. However, this acetate excretion is not observed experimentally (Kohler et al., 2003), providing a strong indication that pyruvate oxidase and acetate kinase are not synthesized in the *hemB* mutant. As such a mutant exists under ''quasi''-fermentative conditions, the lack of synthesis of pyruvate oxidase and acetate kinase should be in line with its regulatory pattern, as these two enzymes are not needed under fermentation conditions. Thus, it can be hypothesized that despite the presence of oxygen, only fermentative pathways are activated in the *hemB* mutant.

Effect of In Silico Gene Deletions

A gene product that is essential for bacterial growth is a potential target for antibacterial chemotherapy. However, experimental methods for determining whether a gene is essential for growth always involve laborious experiments in order to construct a desired genotype. Even though technologies such as in vitro expression technology will remain invaluable tools to identify elements for example of the bacterial infection process (Angelichio and Camilli, 2002), a metabolic model might be a much more economic way to generate a set of rational hypotheses regarding the essentiality of particular genes under a large set of environmental circumstances. FBA has proven to be a versatile tool to determine the effects of variations in the metabolic genotype (Price et al., 2003). Such in silico screenings for gene deletion effects can be performed within a few minutes, including variations in media and growth conditions.

We have carried out such an analysis for the internal reactions of the core metabolic model of *S. aureus* (without the dead-end pathways, see above) using aerobic growth conditions on complex medium as a test case. The employed medium, designed according to a Staphylococcus medium from Difco Laboratories (Bacto Staphylococcus), contained glucose, lactose, and mannitol as carbon sources, all amino acids for which transporters exist, nicotinate and choline as well as the typically employed nitrogen, sulfur, phosphorus sources (NH_3, sulfate, orthophosphate), and metal ions (Zn^{2+}, K^+, Na^+, Mg^{2+}).

The flux balance analysis revealed that the removal of 158 reactions from the model prevented growth. Table IV gives an overview about the distribution of those reactions whose elimination is incompatible with growth.

The number of predicted essential reactions in relation to the total number of reactions in each sub-metabolism allows classifying the sub-metabolisms into flexible or rigid parts. It is obvious that especially the glycan, lipid, cofactor, and vitamin metabolisms are quite rigid and deletions can hardly be compensated by means of alternative pathways and are potential targets for antibiotic action. A complete list of the

Table IV. Number and percentage of lethal deletions in the sub-metabolisms, excluding membrane transport and biomass constituting reactions.

Sub-metabolism	No. of predicted essential reactions	Total no. of reactions in sub-metabolism	Percentage [%]	Classification
Metabolism of proteinogenic amino acids	33	137	24	Flexible
Biodegradation of xenobiotics	0	6	0	Not used for growth
Carbohydrate metabolism	19	97	20	Flexible
Energy metabolism	3	16	19	Flexible
Glycan biosynthesis and metabolism	18	18	100	Rigid
Lipid metabolism	32	54	59	Rigid
Metabolism of cofactors and vitamins	29	60	48	Rigid
Metabolism of non-proteinogenic amino acids	2	8	25	Flexible
Nucleotide metabolism	20	87	23	Flexible

computational gene deletion results is available in the supplementary files.

The results of our gene deletion study can be compared with experimental data on the effect of metabolic gene deletion from the literature (Jana et al., 2000; Ji et al., 2001; Wilding et al., 2000). From these experimental studies, only those genes were considered for comparison for which an according model reaction could unambiguously be identified. The results of the comparison are provided in Table V. In this table, the experimental data are categorized in *lethal* and *defective*, indicating that the gene deletion has resulted in an unviable cell or in a growth-defective phenotype, respectively. For the computational analysis, the phenotype categories are *lethal*, *yield reduction* (corresponding to defective), and *no difference* (indicating that in silico there is no difference between the wild type and the mutant phenotype in terms of growth rate).

Inspection of Table V reveals that all the lethal gene deletions identified experimentally were correctly predicted by our model. This is a strong indication that the experimentally observed lethality of these particular gene deletions has indeed metabolic reasons. Furthermore, the experimentally observed growth-defective phenotype of three more genes was correctly predicted. Another three genes, for which the model did not identify any effect on growth rate, experimentally showed a growth-defective phenotype. This could indicate that an alternative pathway, chosen in the simulation to circumvent the gene deletion, in fact could not be upregulated to a sufficient level in vivo. Finally, three genes were found to be growth-defective in the experiment whose deletion was predicted lethal in the computational analysis. It turned out that the latter false negatives all encode reactions in the purine metabolism, indicating that this sub-metabolism has to be incomplete in the model. In fact, during the model construction process the purine metabolism required extensive addition of reactions from the KEGG pool of putatively assigned genes or other genomic databases such as SEED or TIGR. This supports the view that purine metabolism genes are poorly conserved and that a number of alternative routes might still exist. Future model extension efforts, therefore, should place a special focus on this area.

In summary, the gene deletion analysis provided an extensive list of metabolic genes that are predicted essential since there is no alternative route available to compensate the deletion. Obviously, there are certain limits to the predictive power of this approach, most prominently because a substantial part of the genome has not been annotated so far and thus some of the reactions identified as essential in the currently available model might not be so in reality. On the other hand, we have to point out that in fact a larger number of metabolic genes could be essential for growth. As regulation aspects (such as for example the regulation-related auxotrophy for certain amino acids (Gladstone, 1937)) are not considered in this metabolic model, it is impossible to identify cases in which a pathway proposed in silico to circumvent a specific gene deletion in reality cannot be employed due to the fact that the respective pathway is not

Table V. Comparison of computational predictions on gene deletion effects with experimental data.

Gene	Enzyme	EC	Sub-metabolism	Experimental phenotype	Predicted phenotype	Comment	Reference
murE	UDP-N-acetylmuramoyl-L-alanyl-D-glutamate-L-lysine ligase	6.3.2.7	Peptidoglycan biosynthesis	Lethal	Lethal		Jana et al. (2000)
pyrC	Dihydrooratase	3.5.2.3	Pyrimidine metabolism	Lethal	Lethal		Ji et al. (2001)
murB	UDP-N-acetylmuramate dehydrogenase	1.1.1.158	Aminosugar metabolism	Lethal	Lethal		Ji et al. (2001)
tkt	Transketolase	2.2.1.1	Pentose phosphate pathway	Lethal	Lethal		Ji et al. (2001)
mvaA	Hydroxymethylglutaryl-CoA reductase	1.1.1.34	Biosynthesis of steroids	Lethal	Lethal		Wilding et al. (2000)
qoxB	Menaquinol oxidase	1.9.3.-	Respiratory chain	Defective	Yield reduction		Ji et al. (2001)
yufD	NADH dehydrogenase	1.6.5.3	Respiratory chain	Defective	Yield reduction		Ji et al. (2001)
pgaM	Phosphoglyceromutase	5.4.2.1	Glycolysis/gluconeogenesis	Defective	Yield reduction		Ji et al. (2001)
Pdh	Pyruvate dehydrogenase	1.2.4.1/2.3.1.12	Glycolysis/gluconeogenesis	Defective	No difference	Regulation	Ji et al. (2001)
YpcA	Glutamate dehydrogenase	1.4.1.2	Glutamate metabolism	Defective	No difference	Regulation	Ji et al. (2001)
adh1	Alcohole dehydrogenase	1.1.1.1		Defective	No difference	Regulation	Ji et al. (2001)
purB	Adenylosuccinatelyase	4.3.2.2	Purine metabolism	Defective	Lethal	Model incomplete	Ji et al. (2001)
purC	Phosphoribosyl aminoimidazole-succinocarboxamide synthase	6.3.2.6	Purine metabolism	Defective	Lethal	Model incomplete	Ji et al. (2001)
adk	Adenylate kinase	2.7.4.3	Purine metabolism	Defective	Lethal	Model incomplete	Ji et al. (2001)

induced. Nevertheless, applying this large-scale gene deletion study, rational hypotheses for drug targets can easily be generated. The enzymes for glycan biosynthesis and lipid metabolism seem to be a promising target as these submetabolisms are quite inflexible.

CONCLUSIONS

A validated metabolic network of *S. aureus* N315, which represents an extensive compendium on *S. aureus* metabolism, was able to predict a number of different metabolic phenotypes and could be used to predict the effects of gene deletions on growth behavior. We hope that the model will be a useful guiding tool for potential future experiments to elucidate the interrelationship of bacterial metabolism and resistance. Furthermore, combining this stoichiometric model with transcriptomic and proteomic data in the future should allow a new quality in the analysis of clinically relevant organisms and a more rationalized system-level search for novel drug targets.

NOTE

During the review process, we became aware of another most recently published metabolic model for *S. aureus* N315 (Becker and Palsson, 2005).

The authors are indebted to the invaluable help of Brigitte Berger-Bächi and her group, Giorgia Valsesia, and Greg Cook.

References

Akesson M, Förster J, Nielsen J. 2004. Integration of gene expression data into genome-scale metabolic models. Metab Eng 6(4):285–293.

Alberty RA. 2000. Calculating apparent equilibrium constants of enzyme-catalyzed reactions at pH 7. Biochemical Education 28(1):12–17.

Angelichio MJ, Camilli A. 2002. *In vivo* expression technology. Infect Immun 70(12):6518–6523.

Arakawa H, Shimada A, Ishimoto N, Ito E. 1981. Occurrence of ribitol-containing lipoteichoic acid in *Staphylococcus aureus* H and its glycosylation. J Biochem 89(5):1555–1563.

Baddiley J. 1989. Bacterial cell walls and membranes—Discovery of the teichoic acids. Bioessays 10(6):207–210.

Becker SA, Palsson BO. 2005. Genome-scale reconstruction of the metabolic network in *Staphylococcus aureus* N315: An initial draft to the two-dimensional annotation. BMC Microbiology 5:8.

Blumenthal HJ. 1972. Glucose catabolism in staphylococci. In: Cohen JO, editor. Staphylococci. New York: Interscience. p 111–135.

Bronner S, Monteil H, Prevost G. 2004. Regulation of virulence determinants in *Staphylococcus aureus*: Complexity and applications. FEMS Microbiology Reviews 28(2):183–200.

Burgard AP, Maranas CD. 2003. Optimization-based framework for inferring and testing hypothesized metabolic objective functions. Biotechnol Bioeng 82(6):670–677.

Burke KA, Lascelles J. 1975. Nitrate reductase system in *Staphylococcus aureus* wild type and mutants. J Bacteriol 123(1):308–316.

Burke KA, Lascelles J. 1979. Partial purification and some properties of the *Staphylococcus aureus* cytoplasmic nitrate reductase. J Bacteriol 139(1):120–125.

Burke KA, Brown AE, Lascelles J. 1981. Membrane and cytoplasmic nitrate reductase of *Staphylococcus aureus* and application of crossed immunoelectrophoresis. J Bacteriol 148(2):724–727.

Chen SL. 1964. Energy requirement for microbial growth. Nature 202(493): 1135–1136.

Christian JHB, Waltho JA. 1964. The composition of *Staphylococcus aureus* in relation to the water activity to the growth medium. J Gen Microbiol 35:205–213.

Cordwell SJ, Larsen MR, Cole RT, Walsh BJ. 2002. Comparative proteomics of *Staphylococcus aureus* and the response of methicillin-resistant and methicillin-sensitive strains to Triton X-100. Microbiology 148:2765–2781.

Covert MW, Knight EM, Reed JL, Herrgard MJ, Palsson BO. 2004. Integrating high-throughput and computational data elucidates bacterial networks. Nature 429(6987):92–96.

Cui LZ, Murakami H, Kuwahara-Arai K, Hanaki H, Hiramatsu K. 2000. Contribution of a thickened cell wall and its glutamine nonamidated component to the vancomycin resistance expressed by *Staphylococcus aureus* Mu50. Antimicrob Agents Chemother 44(9):2276–2285.

Dunman PM, Mounts W, McAleese F, Immermann F, Macapagal D, Marsilio E, McDougal L, Tenover FC, Bradford PA, Petersen PJ, Projan SJ, Murphy E. 2004. Uses of *Staphylococcus aureus* GeneChips in genotyping and genetic composition analysis. J Clin Microbiol 42(9): 4275–4283.

Förster J, Famili I, Fu P, Palsson BO, Nielsen J. 2003. Genome-scale reconstruction of the *Saccharomyces cerevisiae* metabolic network. Genome Res 13(2):244–253.

Garrard W, Lascelle J. 1968. Regulation of *Staphylococcus aureus* lactate dehydrogenase. J Bacteriol 95(1):152.

Gladstone GP. 1937. The nutrition of *Staphylococcus aureus*: Nitrogen requirements. Br J Exp Pathol 18:322–333.

Graham JE, Wilkinson BJ. 1992. *Staphylococcus aureus* osmoregulation-roles for choline, glycine betaine, proline, and taurine. J Bacteriol 174(8):2711–2716.

Gutberlet T, Dietrich U, Bradaczek H, Pohlentz G, Leopold K, Fischer W. 2000. Cardiolipin, alpha-D-glucopyranosyl, and L-lysylcardiolipin from gram-positive bacteria: FAB MS, monofilm and X-ray powder diffraction studies. Biochim Biophys Acta 1463(2):307–322.

Hanaki H, Kuwahara-Arai K, Boyle-Vavra S, Daum R, Labischinski H, Hiramatsu K. 1998. Activated cell-wall synthesis is associated with vancomycin resistance in methicillin-resistant *Staphylococcus aureus* clinical strains Mu3 and Mu50. J Antimicrob Chemother 42(2):199–209.

Hancock R. 1960. The amino acid composition of the protein and cell wall of *Staphylococcus aureus*. Biochim Biophys Acta 37(1):42–46.

Harrington C, Baddiley J. 1985. Biosynthesis of wall teichoic acids in *Staphylococcus aureus* H, *Micrococcus* varians and *Bacillus subtilis* W23. Involvement of lipid intermediates containing the disaccharide *N*-acetylmannosaminyl *N*-acetylglucosamine. Eur J Biochem 153(3): 639–645.

Hecker M, Engelmann S, Cordwell SJ. 2003. Proteomics of *Staphylococcus aureus*—Current state and future challenges. J Chromatogr B 787(1): 179–195.

Hugo WB, Davidson JR. 1973. Effect of cell lipid depletion in *Staphylococcus aureus* upon its resistance to antimicrobial agents. 1. Lipid depletion induced by biotin deficiency. Microbios 8(29):43–51.

Iliopoulos I, Tsoka S, Andrade M, Janssen P, Audit B, Tramontano A, Valencia A, Leroy C, Sander C, Ouzounis C. 2000. Genome sequences and great expectations. Genome Biol 2(1): (Interactions 0001.1).

Ingraham JL, Maaløe O, Neidhardt FC. 1983. Growth of the bacterial cell: Sunauer Associates, Inc.

Ito E, Strominger JL. 1962. Enzymatic synthesis of peptide in bacterial uridine nucleotides. 1. Enzymatic addition of L-alanine, D-glutamic acid, and L-lysine. J Biol Chem 237(8):2689–2695.

Jana M, Luong T-T, Komatsuzawa H, Shigeta M, Lee CY. 2000. A method for demonstrating gene essentiality in *Staphylococcus aureus*. Plasmid 44(1):100–104.

Ji Y, Zhang B, Van Horn SF, Warren P, Woodnutt G, Burnham MKR, Rosenberg M. 2001. Identification of critical staphylococcal genes

using conditional phenotypes generated by antisense RNA. Science 293(5538):2266–2269.

Jiang WP, Hermolin J, Fillingame RH. 2001. The preferred stoichiometry of *c* subunits in the rotary motor sector of *Escherichia coli* ATP synthase is 10. Proc Natl Acad Sci U S A 98(9):4966–4971.

Jolly L, Wu S, van Heijenoort J, de Lencastre H, Mengin-Lecreulx D, Tomasz A. 1997. The *femR315* gene from *Staphylococcus aureus*, the interruption of which results in reduced methicillin resistance, encodes a phosphoglucosamine mutase. J Bacteriol 179(17):5321–5325.

Kashket ER. 1981. Proton motive force in growing *Streptococcus lactis* and *Staphylococcus aureus* cells under aerobic and anaerobic conditions. J Bacteriol 146(1):369–376.

Kiriukhin MY, Neuhaus FC. 2001. D-alanylation of lipoteichoic acid: Role of the D-alanyl carrier protein in acylation. J Bacteriol 183(6):2051–2058.

Koch HU, Haas R, Fischer W. 1984. The role of lipoteichoic acid biosynthesis in membrane lipid-metabolism of growing *Staphylococcus aureus*. Eur J Biochem 138(2):357–363.

Kohler C, von Eiff C, Peters G, Proctor RA, Hecker M, Engelmann S. 2003. Physiological characterization of a heme-deficient mutant of *Staphylococcus aureus* by a proteomic approach. J Bacteriol 185(23): 6928–6937.

Kubak BM, Yotis WW. 1981. Analysis of *Staphylococcus aureus* cytoplasmic membrane proteins by isoelectric focusing. Biochim Biophys Acta 649:642–650.

Kuroda M, Ohta T, Uchiyama I, Baba T, Yuzawa H, Kobayashi I, Cui L, Oguchi A, Aoki K-i, Nagai Y. 2001. Whole genome sequencing of meticillin-resistant *Staphylococcus aureus*. Lancet 357(9264):1225–1240.

Kuroda M, Kuroda H, Oshima T, Takeuchi F, Mori H, Hiramatsu K. 2003. Two-component system VraSR positively modulates the regulation of cell-wall biosynthesis pathway in *Staphylococcus aureus*. Mol Microbiol 49(3):807–821.

Lascelles J. 1979. Heme-deficient mutants of *Staphylococcus aureus*. Methods Enzymol p 172–178.

Lascelles J, Burke KA. 1978. Reduction of ferric iron by L-lactate and DL-glycerol-3-phosphate in membrane preparations from *Staphylococcus aureus* and interactions with nitrate reductase system. J Bacteriol 134(2):585–589.

Lowy FD. 2003. Antimicrobial resistance: The example of *Staphylococcus aureus*. J Clin Invest 111(9):1265–1273.

Mahadevan R, Schilling CH. 2003. The effects of alternate optimal solutions in constraint-based genome-scale metabolic models. Metab Eng 5:264–276.

McNamara PJ, Proctor RA. 2000. *Staphylococcus aureus* small colony variants, electron transport and persistent infections. Int J Antimicrob Agents 14(2):117–122.

Miller RD, Fung DYC. 1973. Amino acid requirements for production of enterotoxin-B by *Staphylococcus aureus* S-6 in a chemically defined medium. Appl Microbiol 25(5):800–806.

Miller KJ, Zelt SC, Bae JH. 1991. Glycine betaine and proline are the principal compatible solutes of *Staphylococcus aureus*. Curr Microbiol 23(3):131–137.

Navarre WW, Schneewind O. 1999. Surface proteins of gram-positive bacteria and mechanisms of their targeting to the cell wall envelope. Microbiol Mol Biol Rev 63(1):174–229.

Neuhaus FC, Baddiley J. 2003. A continuum of anionic charge: Structures and functions of D-alanyl-teichoic acids in gram-positive bacteria. Microbiol Mol Biol Rev 67(4):686–723.

Novick RP. 2003. Autoinduction and signal transduction in the regulation of staphylococcal virulence. Mol Microbiol 48(6):1429–1449.

O'Leary WM, Wilkinson SG. 1988. Gram-positive bacteria. In: Ratledge C, Wilkinson SG, editors. Microbial lipids. London: Academic Press. p 117–201.

Papin JA, Stelling J, Price ND, Klamt S, Schuster S, Palsson BO. 2004. Comparison of network-based pathway analysis methods. Trends Biotechnol 22(8):400–405.

Patil KR, Akesson M, Nielsen J. 2004. Use of genome-scale microbial models for metabolic engineering. Curr Opin Biotechnol 15(1):64–69.

Pechous R, Ledala N, Wilkinson BJ, Jayaswal RK. 2004. Regulation of the expression of cell wall stress stimulon member gene *msrA1* in methicillin-susceptible or-resistant *Staphylococcus aureus*. Antimicrob Agents Chemother 48(8):3057–3063.

Perego M, Glaser P, Minutello A, Strauch MA, Leopold K, Fischer W. 1995. Incorporation of D-alanine into lipoteichoic acid and wall teichoic acid in *Bacillus subtilis*- Identification of genes and regulation. J Biol Chem 270(26):15598–15606.

Pereira MP, Brown ED. 2004. Bifunctional catalysis by CDP-ribitol synthase: Convergent recruitment of reductase and cytidylyltransferase activities in *Haemophilus influenzae* and *Staphylococcus aureus*. Biochemistry 43(37):11802–11812.

Perry AM, Ton-That H, Mazmanian SK, Schneewind O. 2002. Anchoring of surface proteins to the cell wall of *Staphylococcus aureus*. III. Lipid II is an in vivo peptidoglycan substrate for sortase-catalyzed surface protein anchoring. J Biol Chem 277(18):16241–16248.

Pramanik J, Keasling JD. 1997. Stoichiometric model of *Escherichia coli* metabolism: Incorporation of growth-rate dependent biomass composition and mechanistic energy requirements. Biotechnol Bioeng 56(4): 398–421.

Pramanik J, Keasling JD. 1998. Effect of *Escherichia coli* biomass composition on central metabolic fluxes predicted by a stoichiometric model. Biotechnol Bioeng 60(2):230–238.

Price ND, Papin JA, Schilling CH, Palsson BO. 2003. Genome-scale microbial *in silico* models: The constraints-based approach. Trends in Biotechnology 21(4):162–169.

Proctor RA, Balwit JM, Vesga O. 1994. Variant subpopulations of *Staphylococcus aureus* as cause of persistent and recurrent infections. Infect Agents Dis 3:302–312.

Reed JL, Vo TD, Schilling CH, Palsson BO. 2003. An expanded genome-scale model of *Escherichia coli* K12 (iJR904 GSM/GPR). Genome Biol 4(9):R54.

Reusch VM, Jr. 1984. Lipopolymers, isoprenoids, and the assembly of the gram-positive cell wall. CRC Crit Rev Microbiol 11:129–155.

Sasarman A, Purvis P, Portelan V. 1974. Role of menaquinone in nitrate respiration in *Staphylococcus aureus*. J Bacteriol 117(2):911–913.

Schilling CH, Covert MW, Famili I, Church GM, Edwards JS, Palsson BO. 2002. Genome-scale metabolic model of *Helicobacter pylori* 26695. J Bacteriol 184(16):4582–4593.

Schleifer KH, Kandler O. 1972. Peptidoglycan types of bacterial cell walls and their taxonomic implications. Bacteriology Reviews 36:407–477.

Sehnalova H, Dadak V. 1976. The influence of MK on the activity of dehydrogenases of *Staphylococcus epidermidis*. Scripta Facultatis Scientiarum Naturalium Universitatis Purkynianae Brunensis 6:97–102.

Sieradzki K, Tomasz A. 1999. Gradual alterations in cell wall structure and metabolism in vancomycin-resistant mutants of *Staphylococcus aureus*. J Bacteriol 181(24):7566–7570.

Somerville GA, Chaussee MS, Morgan CI, Fitzgerald JR, Dorward DW, Reitzer LJ, Musser JM. 2002. *Staphylococcus aureus* aconitase inactivation unexpectedly inhibits post-exponential-phase growth and enhances stationary-phase survival. Infect Immun 70(11):6373–6382.

Somerville GA, Said-Salim B, Wickman JM, Raffel SJ, Kreiswirth BN, Musser JM. 2003. Correlation of acetate catabolism and growth yield in *Staphylococcus aureus*: Implications for host-pathogen interactions. Infect Immun 71(8):4724–4732.

Stelling J, Klamt S, Bettenbrock K, Schuster S, Gilles ED. 2002. Metabolic network structure determines key aspects of functionality and regulation. Nature 420(6912):190–193.

Stephanopoulos G, Aristidou AA, Nielsen J. 1998. Metabolic engineering. Principles and methodologies. San Diego: Academic Press.

Sutcliffe IC, Shaw N. 1991. Atypical lipoteichoic acids of gram-positive bacteria. J Bacteriol 173:7065–7069.

Tempest DW, Neijssel OM. 1984. The status of YATP and maintenance energy as biologically interpretable phenomena. Annu Rev Microbiol 38:459–486.

Throup JP, Zappacosta F, Lunsford RD, Annan RS, Carr SA, Lonsdale JT, Bryant AP, McDevitt D, Rosenberg M, Burnham MKR. 2001. The *srhSR* gene pair from *Staphylococcus aureus*: Genomic and proteomic approaches to the identification and characterization of gene function. Biochemistry 40(34):10392–10401.

Tomasz A. 2000. The staphylococcal cell wall. In: Fischetti VA, Novick RP, Ferretti JJ, Portnoy DA, Rood JI, editors. Gram-positive pathogens. Washington, DC: ASM Press. p 351–360.

Tynecka Z. 1968. Free amino acids of staphylococci. Exper Med Microbiol 20(3):227–232.

Tynecka Z, Malm A. 1996. Cadmium-sensitive targets in the aerobic respiratory metabolism of *Staphylococcus aureus*. J Basic Microbiol 36(6):447–452.

Tynecka Z, Szczesniak Z, Malm A, Los R. 1999. Energy conservation in aerobically grown *Staphylococcus aureus*. Res Microbiol 150(8):555–566.

Varma A, Boesch BW, Palsson BO. 1993. Stoichiometric interpretation of *Escherichia coli* glucose catabolism under various oxygenation rates. Appl Environ Microbiol 59(8):2465–2473.

Vinnikov AI. 1988. ATP synthesis in *S. aureus* cells during the induction of membrane potential and proton gradient. Biokhimiya (Moscow) 53(5): 853–855.

von Eiff C, Heilmann C, Proctor RA, Woltz C, Peters G, Götz F. 1997. A site-directed *Staphylococcus aureus hemB* mutant is a small-colony variant which persists intracellularly. J Bacteriol 179(15):4706–4712.

Ward JB, Perkins HR. 1968. The chemical composition of membranes of protoplasts and L-forms of *Staphylococcus aureus*. Biochem J 106(2): 391–400.

Weerkamp A, Heinenvonborries UJ, Vogels GD. 1978. Biochemical and ultrastructural changes in *Staphylococcus aureus* treated with staphylococcin 1580. Antonie Van Leeuwenhoek J Microbiol 44(1):35–48.

Weidel W, Pelzer H. 1964. Bagshaped macromolecules—A new outlook on bacterial cell walls. Adv Enzymol 26:192–232.

White DC, Frerman FE. 1967. Extraction, characterization, and cellular localization of the lipids of *Staphylococcus aureus*. J Bacteriol 94(6):1854–1867.

Wilding EI, Kim D-Y, Bryant AP, Gwynn MN, Lunsford RD, McDevitt D, Myers JE, Jr., Rosenberg M, Sylvester D, Stauffacher CV, Rodwell WW. 2000. Essentiality, expression, and characterization of the class II 3-hydroxy-3-methylglutaryl coenzyme A reductase of *Staphylococcus aureus*. J. Bacteriol 182(18):5147–5152.

Wilkinson BJ. 1997. Biology. In: Crossley KB, Archer GL, editors. The staphylococci in human disease. New York: Churchill Livingstone. p 1–38.

Wiltshire MD, Foster SJ. 2001. Identification and analysis of *Staphylococcus aureus* components expressed by a model system of growth in serum. Infect Immun 69(8):5198–5202.

Witte W. 1999. Antibiotic resistance in gram-positive bacteria: Epidemiological aspects. J Antimicrob Chemother 44(90001):1–9.

Wu C-H, Bergdoll MS. 1971. Stimulation of enterotoxin B production. Infect Immun 3(6):784–792.